

See discussions, stats, and author profiles for this publication at: <https://www.researchgate.net/publication/311911906>

# NONLINEAR DYNAMIC SOIL-STRUCTURE INTERACTION EFFECTS ON THE SEISMIC RESPONSE OF A PILE-SUPPORTED INTEGRAL BRIDGE STRUCTURE

Conference Paper · August 2016

CITATIONS

2

READS

637

6 authors, including:



[Ali Guney Ozcebe](#)

European Centre for Training and Research in Earthquake Engineering

24 PUBLICATIONS 85 CITATIONS

[SEE PROFILE](#)



[Kaustubh Dasgupta](#)

Indian Institute of Technology Guwahati

84 PUBLICATIONS 195 CITATIONS

[SEE PROFILE](#)



[Arindam Dey](#)

Indian Institute of Technology Guwahati

278 PUBLICATIONS 775 CITATIONS

[SEE PROFILE](#)

Some of the authors of this publication are also working on these related projects:



SINAPS@ [View project](#)



Raft Foundations [View project](#)



## NONLINEAR DYNAMIC SOIL-STRUCTURE INTERACTION EFFECTS ON THE SEISMIC RESPONSE OF A PILE-SUPPORTED INTEGRAL BRIDGE STRUCTURE

**Sreya Dhar**

IIT Guwahati  
Guwahati, India

**Ali Güney  
Özcebe**

Politecnico di  
Milano, Italy

**Kaustubh  
Dasgupta**

IIT Guwahati  
Guwahati, India

**Arindam Dey**

IIT Guwahati  
Guwahati, India

**Roberto  
Paolucci**

Politecnico di  
Milano, Italy

**Lorenza  
Petrini**

Politecnico di  
Milano, Italy

### ABSTRACT

Nonlinear dynamic soil structure interaction of a pile-supported integral bridge structure has been reported in this paper. The open source code: OpenSeesSP (parallel processing) have been used to simulate the sequential steps of the analysis. Development of a soil-foundation-structure model was required to properly simulate seismic wave propagation through linear/nonlinear soil. Considering linear and nonlinear soil material behavior, 1D site response analyses have been conducted in time domain using DEEPSOIL software. Two-dimensional numerical analyses, simulating the seismic response of (1) free field soil, (2) soil with pile foundation +model (SWF) and (3) a full soil-foundation-bridge (SFB) system, were carried out based on the propagation of relevant spectrum-compatible natural rock outcrop ground motions (selected and scaled using REXEL-Disp software). It is observed that the effect of soil nonlinearity on the linear structural response can be significant when subjected to high intensity ground motions. Results also indicate that free field motions may differ significantly from that observed under the base of the bridge foundations, indicating that the use of free field motions as input at the base of the bridge piers might not be always justifiable.

### INTRODUCTION

Seismic waves propagating through the soil media and reaching the foundation of structure causes it to shake, subsequently resulting in the vibration of the superstructure (JSCE, 1985). The dynamic characteristics of input ground motion at the base of the structure depend upon the amplification or de-amplification of the bedrock motion propagating through the intervening soil strata. Thus, the knowledge of wave propagation through the soil medium helps to understand the characteristics of the ground motion modifications. Referring in particular to the extended structures, as bridges, literatures reported the modeling of the foundation soil explicitly in order to better represent the dynamic soil-structure interaction (SSI) mechanism (Clough and Penzien, 2003). In their comprehensive study, McCallen and Romstad (1994) developed a detailed nonlinear (material) three-dimensional FE model of an actual soil-foundation-bridge system and modeled explicitly the soil and pile group foundations. Kontoe (2006) carried out time integration schemes and advanced boundary conditions for dynamic geotechnical problems. Maheshwari et al. (2004) performed 3D finite element nonlinear dynamic analysis of pile groups

for lateral and seismic excitations. Although it is known that soil-structure interaction results in a significant modification of the dynamic system properties, the scarcity of pertinent experimental data and the lack of an efficient way to apply the design procedure enhances the complexity of the problem. As a result, often in seismic design or assessment, SSI and/or nonlinear soil response are disregarded.

The aim of this work is to shed some further light onto the effects of only bridge and bridge with explicit soil model approaches on the study of the seismic response. In particular, a bridge structure geometrically resembling the Humboldt middle channel bridge (Humboldt County, California USA) has been considered. In the past, two dimensional and three dimensional analyses of this bridge have been performed considering sophisticated non-linear SSI models (Zhang et al, 2008 and Elgamal et al, 2008). Herein, the seismic response of the bridge (assumed linear elastic for the sake of simplicity) in case of SSI with linear and nonlinear soil models and the response at the free field with that of the whole Soil-Foundation-Bridge model (SFB) is compared.

## DESCRIPTION OF MODEL

As illustrated in detail in Zhang et al. (2008), the Humboldt Bay Middle Channel Bridge is located near Eureka in California, USA. The bridge is 332m long, 10m wide, and 12m high (average height over mean water level). The bridge superstructure consists of nine spans with four precast prestressed concrete I-girders and cast-in-place concrete slabs. The bridge deck is supported by two seat-type abutments and eight bents consisting of a single column and hammer head cap beam. The third and sixth bents have nonlinear shear keys for energy dissipation. Though only linear elastic properties have been used to model the bridge superstructure in the present study. Pile caps of 1m thickness are supported by deep foundations consisting of driven precast prestressed concrete pile groups. For the sake of simplicity, only the longitudinal dynamic response was analyzed in this study. However, the out-of-plane response might be significantly important to investigate in broader aspect of SSI response.

### Soil and foundation models

Two dimensional soil modeling has been carried out in OpenSeesSP (McKenna, 2008). Modelling parameters have

been taken from Zhang et al. (2008). Soil domain is 1500m wide (evaluated through iterations) and 220m in depth (Fig. 1). Whole soil domain consists of 4 different layers (Figure 2) having the properties summarized in Table 1. Pile group stiffness has been analyzed according to Mokwa and Duncun (2000) and modeled as an equivalent pile group. Pile groups are spread to 7m in the out of plane direction. Thus, a thickness of 7m was selected for the soil domain. It should be noted that the soil thickness, even in out of plane direction, contributes mass to the overall longitudinal dynamic analysis (Zhang et al., 2008). Pressure independent multi-yield material has been used to describe the soil behavior through a formulation based on the multi-surface plasticity concept with associative flow rule, inbuilt in OpenSees. The yield surfaces are of the Von Mises type (Prevost, 1985). Since total stress analyses have been carried out, any direct consequence of significant excess pore water pressure generation has been naturally neglected in the present study. For soil domain nonlinearities, variation of shear modulus degradation and damping ratio with shear strain is adopted as per the proposition of Darendeli (2001), which are shown in Fig. 3a. and 3b, respectively.

Table 1. Properties of different soil layers used in the present study (modified after Zhang et al., 2008)

Soil layer	Elastic properties			Non-linear properties		
	$G_{max}$ (MPa)	Poisson's ratio ( $\nu$ )	Total unit weight ( $t/m^3$ )	Undrained strength (kPa)	$G/G_{max}$ Fig. 3(a)	Plasticity Index (PI)
OL/SM	76	0.45	1.9	30	Black Line	10
SP/SM	171	0.45	1.9	11.9	Red Line	0
CL	288	0.45	1.8	100	Blue Line	30
SP	525	0.45	2.1	52.5	Purple Line	0

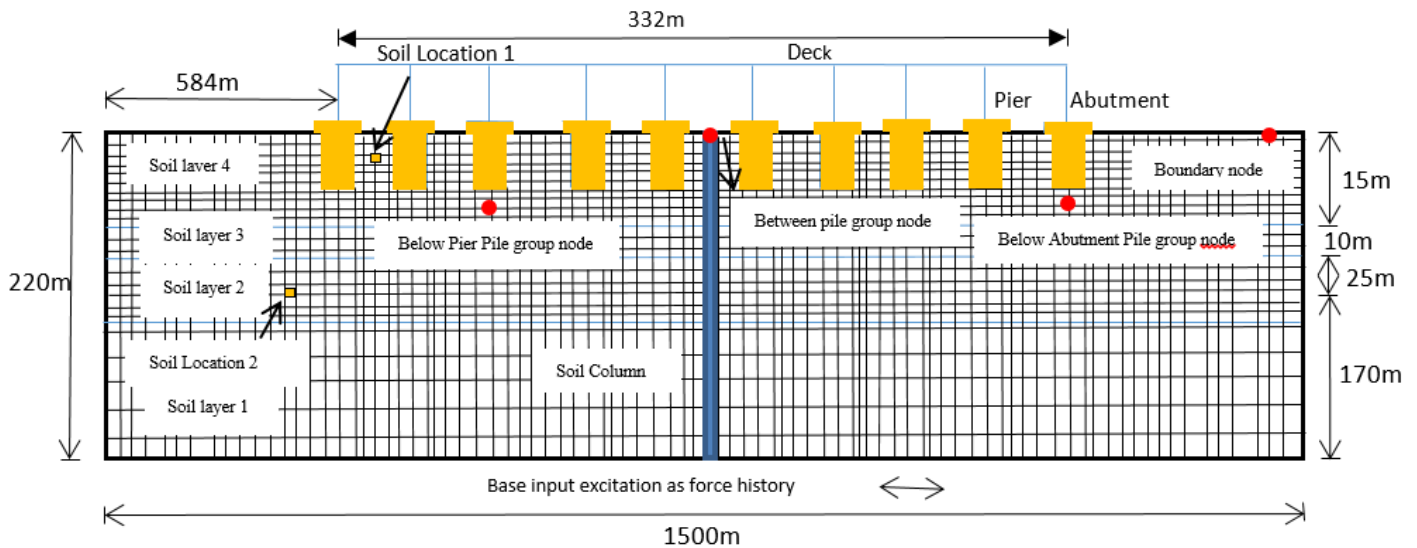


Fig.1 Mesh grid discretization of soil domain (not-in-scale) and overall soil-structure model in OpenSeesSP

The soil domain lateral boundary conditions have been implemented by tied degrees of freedom (TDOF) (Elgamal et al., 2008; Kontoe et al., 2007) at the lateral two ends of the domain. This implies that the soil domain follows the pattern of a 2D shear beam, in which generally the horizontal response is predominant than vertical response. At the base level, classical Lysmer and Kuhlemeyer (1969) type absorbing boundary conditions have been applied in horizontal direction by properly calibrating the dashpot coefficients together with the classical vertical displacement restraints. The dynamic base input motion has been given in horizontal direction in order to study the horizontal response of soil-structure system.

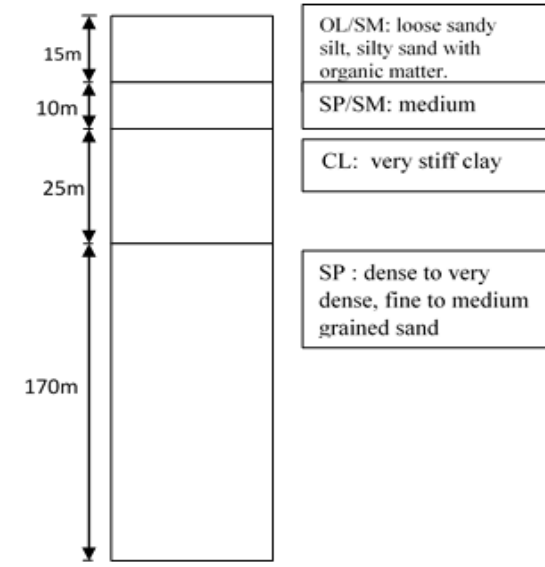


Fig.2 Modified 1D Soil column with soil classification (Zhang et al., 2008)

Soil domain has been modeled by four-noded quadrilateral (quad) elements. The mesh dimension has been determined so that seismic waves can accurately propagate with a maximum frequency of 15 Hz. Accordingly, soil mesh (Fig. 1) was reduced moving from bottom to top from 5m to 1m length [ $L_{max} = V_s / 8f_{max}$ , where  $L_{max}$  is the maximum length of soil mesh,  $V_s$  is the mean shear wave velocity and  $f_{max}$  is the maximum frequency to be propagated by the soil mesh (Kuhlemeyer and Lysmer, 1973)]. Piles are also modelled by 4 four-noded quad elements with properties of reinforced concrete. No interface elements between the structural and soil elements have been used in the present study thus, a rigid soil-pile contact is assumed for the analysis.

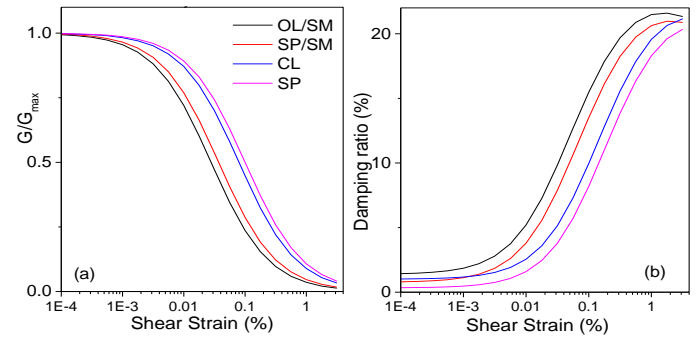


Fig. 3(a) Shear modulus vs. Shear strain curves for different soil layers, (b) Damping ratio vs. Shear strain curves for different soil layers (Darendeli, 2001).

### Superstructure model

The bridge superstructure has been modelled by elastic beam-column elements with continuous joints. The properties of the elements (Table 2) have been taken from Zhang et al. (2008). From the 3D properties of bridge deck equivalent 2D properties have been calculated and used for 2D analysis in OpenSees. The concrete grade is considered as M30.

Table 2. Properties of bridge superstructure and substructure

Members	Area(m <sup>2</sup> )	Young's Modulus, Es (MPa)	Moment of inertia Iz (m <sup>4</sup> )
Abutments	11	28000	1.1092
Beams	4.562	28000	4.30
Piers	3.4	28000	0.8188

### VALIDATION OF LINEAR/NONLINEAR SOIL DOMAIN IN OPENSEES WITH DEEPSOIL

For 1D linear and non-linear analyses in time domain, results from DEEPSOIL v5.1 (Hashash et al., 2015) has been used to validate the same obtained from OpenSees. The two codes differ in the description of nonlinear modelling of soil domain; as mentioned, Opensees considers nested plasticity concept, while in DEEPSOIL a backbone curve is accompanied with unloading and reloading curves. Modified hyperbolic model is adopted to represent the backbone curve of the soil along with the extended unloading-reloading Masing rules (Masing, 1926) to model hysteretic behavior (Hashash et al., 2010). Masing rules (Masing 1926) and extended Masing rules (Pyke, 1979; Vucetic, 1990) are used in conjunction with the backbone curve to describe the energy dissipation characteristics (i.e., damping ratio) and cyclic shear modulus

degradation behavior of soil. A soil column (Fig. 2) was considered in both codes, in which the soil parameters, i.e., soil and bedrock properties, have been kept the same as far as possible (Table 1). A Rayleigh damping scheme has been introduced to model viscous material properties at small strains. Specifically, to calibrate the Rayleigh damping

parameters, the damping ratio was prescribed as 2% at 0.2Hz and 20Hz, for both OpenSees and DEEPSOIL. With PGA of 0.2g Ricker wavelet (with  $f_{max}=2\text{Hz}$  and maximum amplitude at  $t_0=1\text{sec}$ ) has been given as bedrock input motion.

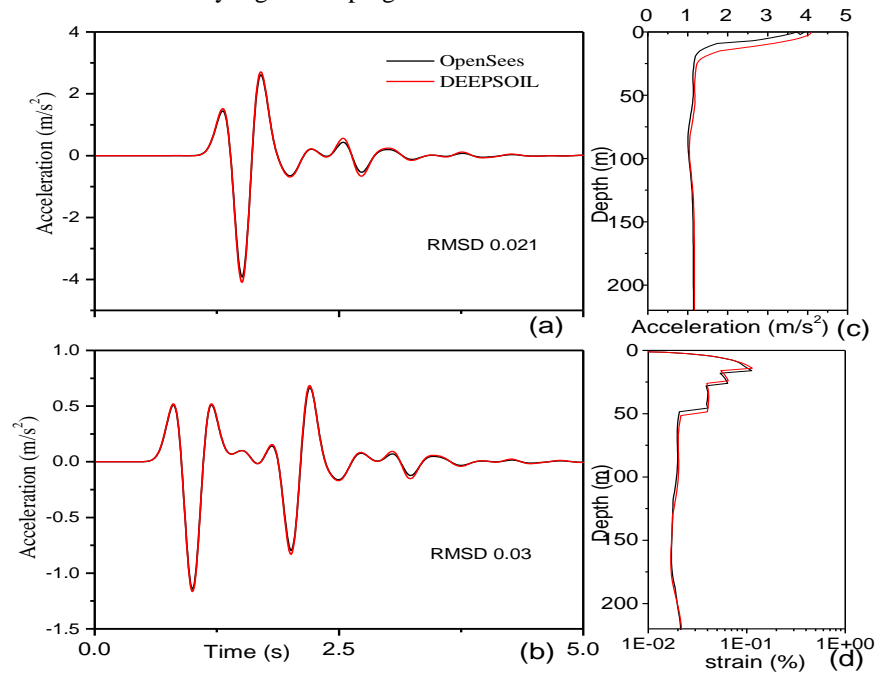


Fig. 4 Linear soil column analyses: (a) Acceleration time history of soil column at 5m from the base, (b) acceleration time history of soil column at surface, (c) maximum acceleration profile, (d) max strain profile throughout the depth of column

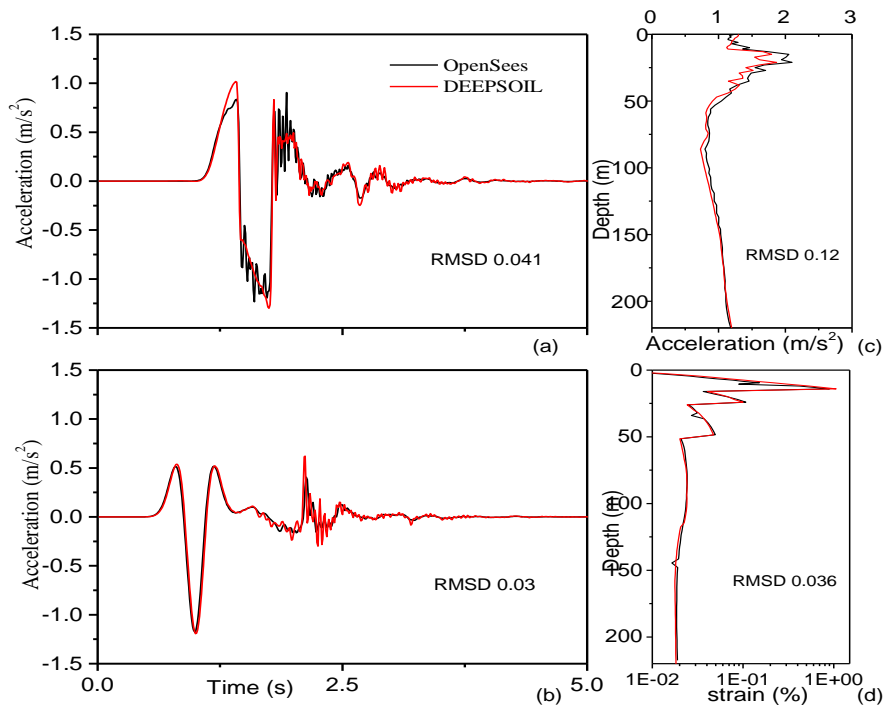


Fig. 5 Nonlinear soil column analyses: (a) Acceleration time history of soil column at 5m from the base, (b) acceleration time history of soil column at surface, (c) maximum acceleration profile, (d) max strain profile throughout the depth of column

The acceleration time histories, maximum acceleration and strain profiles are shown for the linear (Fig. 4) and nonlinear (Fig. 5) models at 5m depth and at ground surface. A good match is obtained for linear analyses (Fig. 4). On the other hand, it is shown that a reasonable agreement is found for nonlinear analyses, having the root mean square deviation (RMSD) of 0.041, 0.12 and 0.036, respectively (Fig. 5). It should be remarked that high frequency disturbances appear in results obtained from both the codes. This effect may be reduced by increasing the mesh fineness in the zones in which the nonlinearity is occurring and post-processing the output time histories with a proper zero-phase filter.

## OPENSEES DYNAMIC SSI ANALYSES

### Selection of Ground Motions

A bedrock uniform hazard response spectrum (UHRS) was used to select input motions for the analyses. The

UHRS was developed from the 2008 United States Geological Survey (USGS, 2008) national seismic hazard maps for the Humboldt Bay area for rock outcrop assuming  $V_{s, 30m} = 800\text{m/s}$  (according to NEHRP (Holzer et al., 2005), site class B). The corresponding 5% damped elastic displacement response spectrum has been given as target to REXEL-Disp (Smerzini et al., 2012) to select the ground motions for dynamic analysis from strong ground motion database SIMBAD (Smerzini et al., 2014). The input parameters in REXEL-Disp to find the ground motions are: magnitude = 5.5-7.5; fault to site distance = 0-30km; spectrum matching tolerance =  $\pm 20\%$ ; spectrum matching period = 0.2s-5s; site specification = EC8 site class A; probability of exceedence = 10% in 50 years, representing the return period of 475 years. Seven real record ground motions have been chosen for horizontal direction by scaling in the response spectrum around the period of interest, such that the mean spectral response lies between the tolerances. The corresponding 5% damped elastic displacement spectra with the average of the ground motions are plotted in Figure 6.

Table 3. Different parameters of selected ground motions

Station ID	Earthquake Name	Date	Mw	Fault Mechanism	Epicentral Distance, km	PGA, $\text{m/s}^2$	SF	Scaled PGA, $\text{m/s}^2$	EC8 Site class	Component
ALT	Irpinia	23 Nov 1980	6.9	normal	23.77	0.54	6.31	3.46	A	y
ST_106	South Iceland	17 Jun 2000	6.5	strike-slip	5.25	3.39	0.90	3.06	A	y
ST_112	Olfus	29 May 2008	6.3	strike-slip	8.25	3.28	1.67	5.47	A	y
ST_101	Olfus	29 May 2008	6.3	strike-slip	7.97	5.00	1.41	7.06	A	x
BSC	Irpinia	23 Nov 1980	6.9	normal	28.29	0.95	0.72	0.68	A	y
ST_106	South Iceland	21 Jun 2000	6.4	strike-slip	21.96	0.51	1.42	0.73	A	x
LPCC	Christchurch	21 Feb 2011	6.2	reverse	1.48	9.16	1.38	12.64	A	y
mean values:			6.5		13.85	3.26	1.98	4.73		

### Time history analyses

Before each nonlinear dynamic analysis, a staged static analysis has been carried out. As a first step, to minimize the numerically induced plastic deformations, initialization of stresses due to the self-weight has been carried out by considering a purely linear soil behavior. Then, the soil constitutive relation has been updated to nonlinear and adequate time stepping has been provided for further stabilization of the static stresses. After that, finally, the preselected earthquake ground motion has been applied at the bottom of soil domain. Selected scaled natural rock outcrop horizontal acceleration motions are converted to the corresponding shear stress histories such that resulting shear

waves can propagate upward (into the mesh) and downward (into the absorbent boundaries). Down-going waves are successfully absorbed by the dynamic boundaries located at the base level by making sure that only present waves in the model are the one that are realistically up-going (incident) shear waves from base of soil domain.

At different locations of the soil domain (Fig. 7(L)), the soil response has been investigated. However, only results of two out of the seven rock outcrop recorded earthquake ground motions with PGA of  $0.35g (=3.46 \text{ m/s}^2)$  and  $0.073g (=0.73 \text{ m/s}^2)$  (Table 3) shown in Fig. 8 are discussed to investigate the dynamic soil response of free field and SFB model.

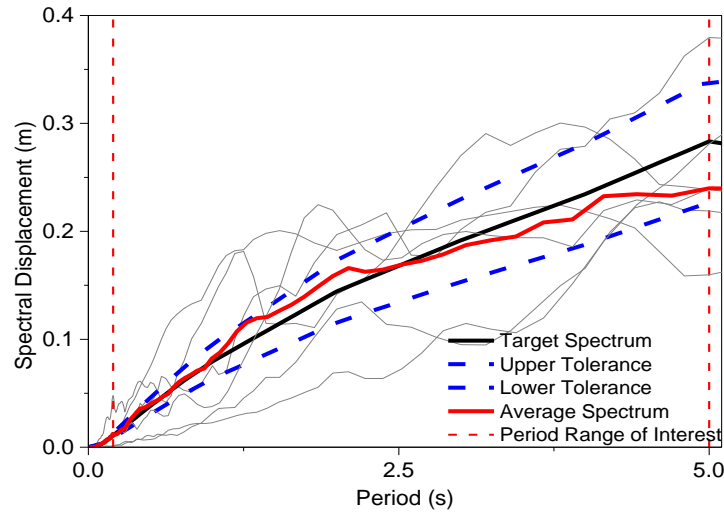


Fig. 6 Displacement Spectra of all the ground motions used in present study.

## RESULTS OF NONLINEAR/LINEAR ANALYSES

Figure 1 shows the locations of a control soil column between pile groups and two soil elements (at locations 1 and 2), at which the soil response is examined. Fig. 7(R) shows the shear stress vs. shear strain hysteretic response at locations 1 and 2 in the foundation soil during GM #1 & #2. The hysteresis loops at the two soil locations 1 and 2 are very narrow for GM #2, indicating low level of inelasticity while during GM #1 the soil response is highly nonlinear. For both the ground motions, soil stresses and strains increase with depth. Response has been shown after the nonlinear gravity analysis, so there is some initial response and after dynamic analysis some residual response is observed for soil. The residual response will depend on soil material property, depth of soil element and base input motion. After the GM #1, the soil element at location 1 and 2 have residual shear strains of 0.06% and 0.11% respectively. While for GM #2 these shear strain values are only 0.012% and 0.07%. This shows that due to high intensity of PGA during the earthquake and high residual response after the GM #1, soil is showing higher inelastic response after dynamic analysis.

Figures 8 shows the profiles for the peak total horizontal acceleration along the height of the one investigated soil column (see Fig. 1) during GM #1 and GM #2 for the three different soil domain cases. The idea of soil column has

been represented from Zhang et al., 2008. For GM #1 (Fig. 8a), the PGA is around  $1.25-1.75\text{m/s}^2$ , which shows de-amplification from the base to 175m depth. Then non-uniform amplification occurs up to 15m depth. Afterwards it again de-amplified near the 15m of soil surface with around PGA  $1.02\text{m/s}^2$ , which is almost similar to free field PGA profile. During GM #2, in soil column 1, it is observed that the acceleration response amplifies and then de-amplifies in a narrow range as the seismic waves travel upwards due to increasing nonlinearity from 220-75m depth. From 75-30m depth the acceleration response amplifies gradually until a reduction is observed from depth between 25-15m. Then it started amplifying again up to soil surface. The acceleration peak is in the range  $0.25-0.5\text{m/sec}^2$  at the base of the soil domain and  $0.7-0.75\text{m/sec}^2$  at the ground surface after significant amplification (Fig. 8b). It is interesting to observe that the presence of bridge foundation adds further reflections on the soil response eventually reducing the peak acceleration with respect to the free field. Fig. 8c and 8d show the shear strain profile of the soil column for GM #1 and GM #2, respectively. For GM #1 the shear strain profile follows the same trend like as GM #2 throughout the depth; though magnitude is not same. On the contrary, for GM #2 SFB model shear strain varied significantly from the FF and SWF model from the depth of 50m to soil surface due to differential nonlinearity in soil layers.

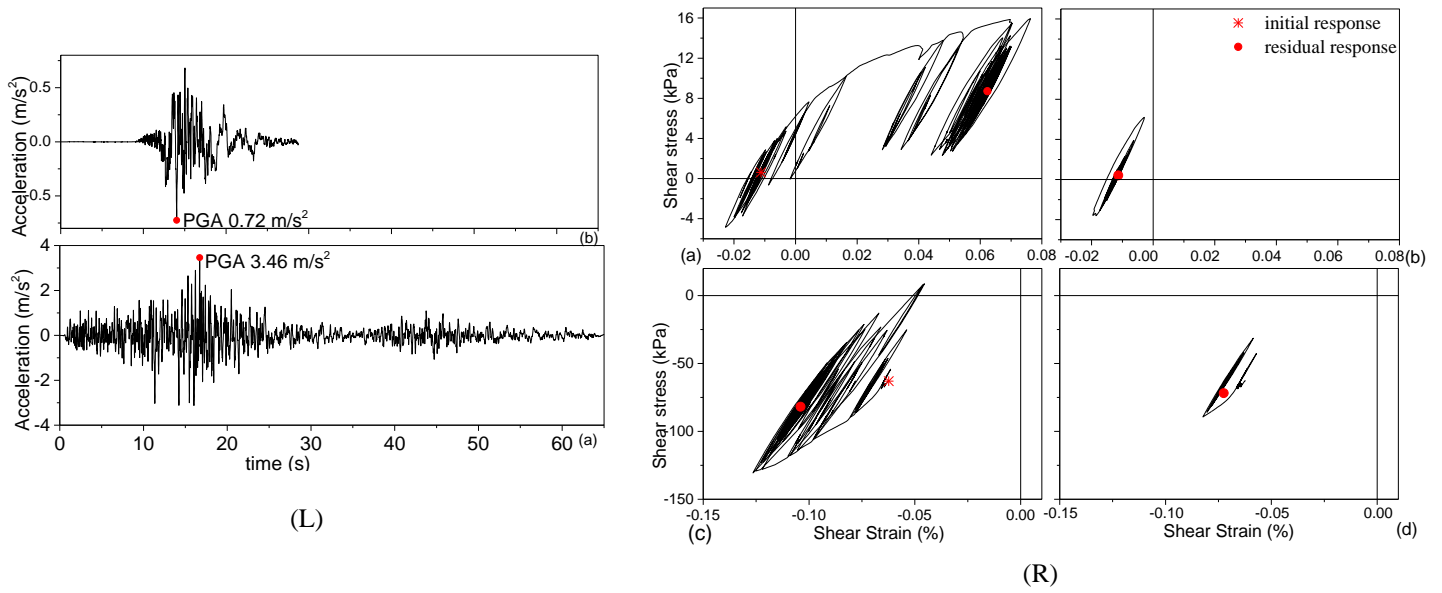


Fig. 7 (L) Rock outcrop earthquake (scaled) records used in this study: (a) normal fault of the 23 Nov. 1980 Irpinia Earthquake,  $M_w=6.9$ , recorded at the 2.77km from epicenter, station ID ALT; Ground Motion (GM) #1 (b) strike-slip fault of the 21 June 2000 South Iceland Earthquake,  $M_w=6.4$ , recorded at the 21.96km from epicenter, station ID ST\_106; Ground Motion (GM) #2. (R) Shear stress vs. shear strain hysteretic response at soil locations 1 and 2: (a) soil location 1, GM #1, (b) soil location 1, GM #2, (c) soil location 2, GM #1, (d) soil location 2, GM #2.

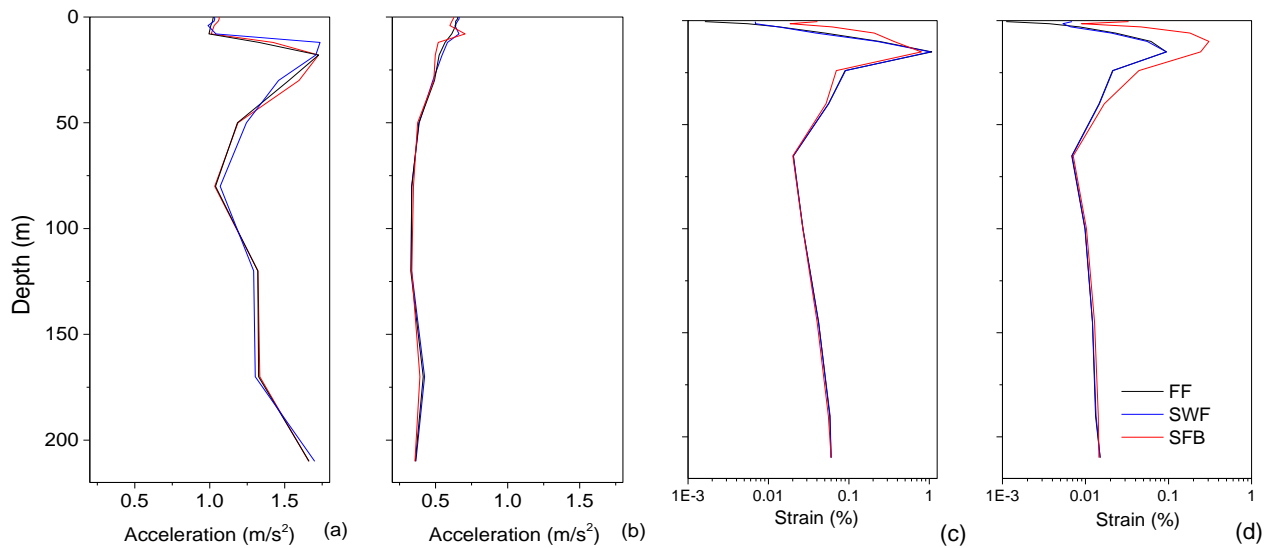


Fig. 8 Comparison of profiles along the height of soil column #1, of peak total horizontal acceleration for (a) GM #1 and (b) GM #2; of peak shear strain for (c) GM #1 and (d) GM #2.



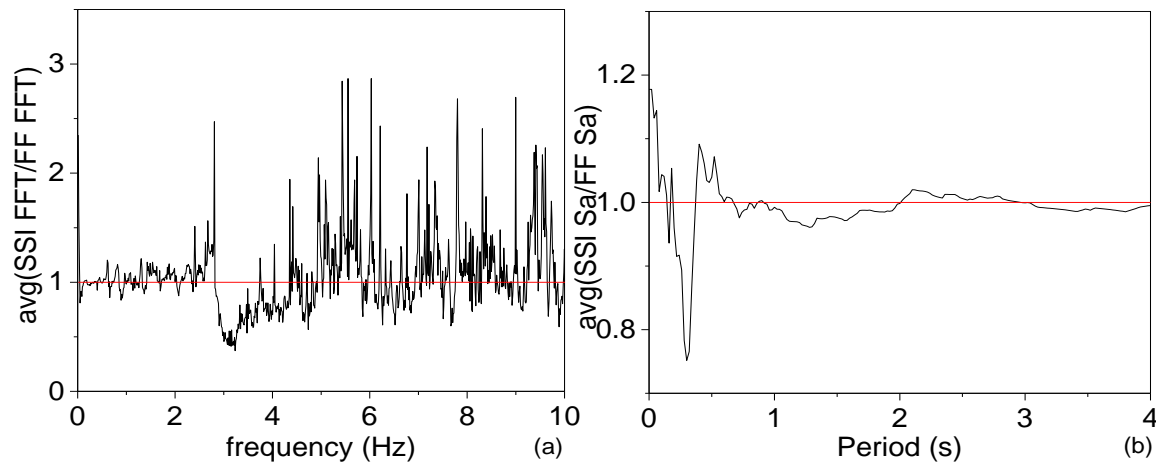


Fig. 9 Comparison of average normalized values at the bottom of pier level and free field values at the foundation level for (a) absolute FFT and (b) 5% damped spectral acceleration.

Figure 9 shows the normalized values of Fourier amplitude and 5% damped acceleration response spectra at the bottom of pier level and free field values at the foundation level to investigate the deviation on input ground motion at the base of the pier from free field motion in the presence of soil. From Fig. 9a, it's visible that the frequency content at the base of bridge pier in SFB model is higher than that of FF model for frequencies greater than 5 Hz and there is a tendency of having lower content between  $f=2-5$  Hz. On the other hand, from Figure 9 (b), it is noted that the presence of bridge alters the spectral response until  $T=1$  sec. Given that, due to the connection type and mass/stiffness characteristics of the only bridge model, the first natural period of vibration also lies in the interval of  $T=0-1$  s. Noting these deviations, the conventional approach of conducting two separate dynamic analyses for site and structural seismic responses could be effectively criticized.

In Fig. 10, the soil domain responses at the node between the pile group (Fig. 10a) below pile group (Fig. 10b) and near the boundary node (Fig. 10c) have been compared with the free field (FF) response for GM #1. At the boundary the soil total displacement time history for SFB system and free field domain are perfectly matching showing the good definition SFB model dimensions. In the node between the pile groups and below the pile group displacement time

histories are different. Hence, analyzing a structure putting only the free field response from soil surface at the base of structure would not suffice for realistic soil-structure behavior as the soil response can get changed in presence of embedded foundation, which is already pointed out in Figure 9. The horizontal displacement response histories at the base of all pile groups are shown in Fig. 11 for GM #1 and #2. Most of the pile group base nodes are displaced permanently towards the right lateral boundary of soil domain due to soil inelasticity induced by reduction in soil shear strength caused by the GM #1. At the end of GM #1, the right abutment pile group moves few centimeters (around 6-7cm) at right while the left abutment pile group moves less than 1.5cm. Due to mild shaking at the end of GM #2 the residual displacements at the base of the pile groups are almost negligible (Fig. 11b). Residual displacement at the end of dynamic analysis also depends upon the base excitation.

The horizontal soil displacement time histories at the locations corresponding to different nodes in the soil structure model due to linear and nonlinear soil properties have been shown and compared in Fig. 12 for GM #1. The residual displacements of non-linear model are 4.7cm and 6.7cm (Fig. 12 (a) and (b) respectively). Due to additional stresses from the abutment mass, the soil below is getting a highly nonlinear inelastic behaviour, resulting in higher residual displacement. Backfill soil has not been modelled in the current study.

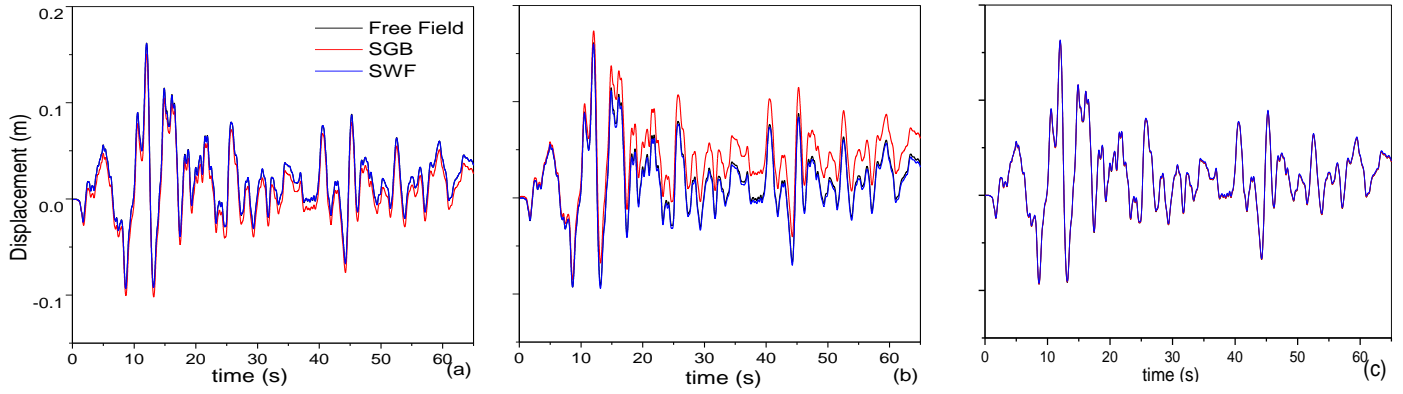


Fig. 10 Total horizontal soil displacement response histories (a) at soil surface between two pile group, (b) below the pile group node and (c) near boundary node due to GM #1.

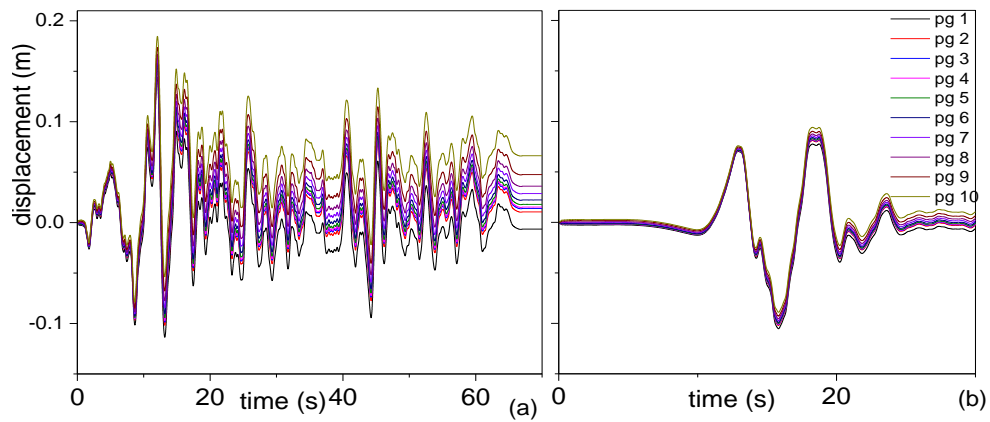


Fig. 11 Total horizontal soil displacement response histories at base of pile groups for (a) GM #1, (b) GM #2

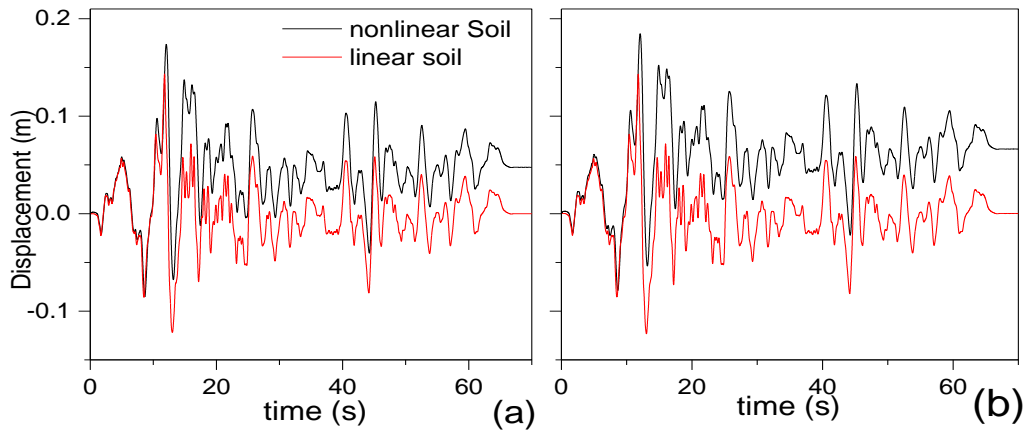


Fig. 12 Total horizontal soil displacement response histories for linear and nonlinear soil domain analysis due to GM #1 at locations (a) below pier pile group node and (b) below abutment pile group node.

## PEAK DYNAMIC RESPONSE OF SFB AND FREE FIELD MODELS

From the above results in the previous sections, it is observed that the dynamic response of FF and SWF models do not differ significantly. So peak dynamic responses of SFB and FF

models considering linear and nonlinear soil properties have been investigated by analysing the models with all the seven rock outcrop recorded ground motions. For the linear soil domain peak mean acceleration is around 4.5-5.5 m/s<sup>2</sup>, while for nonlinear soil domain it is 0.96-1.1 m/s<sup>2</sup>. The mean peak responses in terms of displacement and acceleration are reported in Table 4. No significant difference is noted in terms of average of the peak response quantities (i.e. maximum horizontal displacement, maximum horizontal acceleration) computed for seven individual GMs. Comparing the peak acceleration values in linear and nonlinear cases, the peak in linear conditions is almost 5.7 times higher than in nonlinear soil domain. This shows significant nonlinearity in soil behaviour and high plasticity is observed in some of the soil layers (especially, soil layers 2 and 3). Furthermore, after investigating the high amplitude ratio of peak acceleration in linear and nonlinear soil domain, it should be kept in mind that that liquefaction is likely to occur in sandy soil layers below

foundation. Mean peak displacement is equal or higher in all the cases in nonlinear soil domain compared to linear one. As an outcome of increased soil plasticity, peak mean displacement is highest below the pile group, which is around 18 cm. For both the linear and nonlinear soil domain cases, the boundary response is almost the same. Away from the boundary as the locations are approaching the bridge foundation, the deviation from the free field soil response gets prominent. Thus, according to the response simulation results obtained using the two-dimensional FE model presented here, the seismic response of the bridge in its longitudinal direction is mostly driven by the nonlinear response of the underlying soil. The seismic response mechanism of the bridge shown here would be difficult to be predicted without explicit modelling of the local soil conditions and inelastic behaviour of the soil materials. However, all results presented here are preliminary, and should be corroborated by mesh sensitivity analyses.

Table 4. Peak dynamic response of free field and SFB models

Locations	Soil Property	Model	Average maximum horizontal displacement (m)	Average maximum horizontal acceleration ( m/s <sup>2</sup> )
<i>Near Boundary</i>	linear	free field	0.12	5.6
		SFB	0.12	5.6
	Nonlinear	free field	0.12	1.0
		SFB	0.12	1.0
<i>Below Pile Group</i>	linear	free field	0.12	4.7
		SFB	0.12	4.8
	Nonlinear	free field	0.14	1.0
		SFB	0.18	1.1
<i>Between Pile Group</i>	linear	free field	0.12	5.5
		SFB	0.12	5.5
	Nonlinear	free field	0.13	1.0
		SFB	0.12	1.1

## SUMMARY

Different approaches have been considered to study the effect of dynamic soil-structure interaction effects on the seismic response of a pile supported integral bridge structure, making reference to the Humboldt Bay Middle Channel Bridge, which was already analysed in previous studies (Elgamal et al., 2008; Zhang et al., 2008). Specifically, after considering as a verification the case of free field motion, linear and non-linear models of both the soil-foundation and soil-foundation-structure systems were analysed. A summary of the main conclusions of this study is presented below:

1. A reasonably good match from 1D site response analysis was obtained with DEEPSOIL and OpenSees codes, both for PGA and peak shear strain profiles.
2. The selection of input ground motions from the REXEL-Disp software provided a set of real records

- matching in a broad band sense the target displacement spectrum.
3. By comparing the results of free field (FF) and soil with foundation (SWF) models, it was found that kinematic interaction effects were negligible, while, considering the model including also the structure (SFB model), differences become important, because of inertial interaction effects.
4. Due to soil nonlinearity, there has been significant changes in PGA and peak shear strain profile of the investigated column between FF and SFB model. Due to high levels of non-linearity of the soil below the foundation, it was found that the seismic demand on the superstructure was substantially modified, with additional kinematic effects due to significant residual displacements of the bridge foundations.
5. It is shown that the uncoupled analysis of site response followed by the analysis of structural response by using previously computed free-field

motion may lead to inaccurate results. Depending on the natural vibration characteristics of the structure under consideration, mentioned inaccuracy may be in over- or under-conservative sides.

## ACKNOWLEDGEMENT

Part of this research was carried out while the first author (SD) was visiting Politecnico di Milano, under INTERWEAVE Project, Erasmus Mundus Programme during 2014-2015. The first author would like to thank all the co-authors from PoliMi for their kind co-operation while carrying the research from IITG after end of scholarship period. The first author would like to thank Ministry of Human Resources (MHRD) for the scholarship during PhD work.

## REFERENCES

1. Clough, R. and Penzien, J. (2003), "Dynamics of Structures", 3rd edition, Computers and Structures Inc., Berkeley, California.
2. Darendeli, M. B. (2001), "Development of a new family of normalized modulus reduction and material damping curves". *Ph.D Thesis*, The University of Texas. Austin, Texas.
3. Elgamal, A., Yan, L., Yang, Z. and Conte, J.P. (2008), "Three- Dimensional Seismic Response of Humboldt Bay Bridge-Foundation-Ground System", *Jr. of Struct. Eng.*, ASCE, Vol. 134(7): 1165- 1176.
4. Hashash, Y.M.A., Phillips, C., Yang, Z. and Groholski, D. R. (2010), "Recent advances in Nonlinear site Response Analysis", in *5th International Conference on Recent Advances in Geotechnical Earthquake Engineering and Soil Dynamics*, San Diego, California, USA.
5. Hashash, Y.M.A., Musgrove, M.I., Harmon, J.A., Groholski, D.R., Phillips, C.A., and Park, D. (2015) "DEEPSOIL 6.1, User Manual". Urbana, IL, Board of Trustees of University of Illinois at Urbana-Champaign
6. Holzer, T. L., Padovani, A. C., Bennett, M. J., Noce , E. T. and Tinsley, J. C. (2005), "Mapping NEHRP V<sub>S30</sub> Site Classes", *Earthquake Spectra*, Vol. 21(2): 1-18.
7. Idriss, I. M. (1990), "Response of soft soil sites during earthquakes", in *Proceedings, H. Bolton Seed Memorial Symposium*, J. M. Duncan (editor), vol. 2, BiTech Publishers, Vancouver, British Columbia, 273-289.
8. JSCE (1985), "Dynamic Analysis and Earthquake Resistant Design" by *Japanese Society of Civil Engineers*; Vol. 2, Methods of Dynamic Analysis, Oxford and IBH Publishing Co. Pvt. Ltd.
9. Kontoe, S. (2006), "Development of time integration schemes and advanced boundary conditions for dynamic geotechnical analysis", *PhD thesis*, Imperial College, London.
10. Kontoe, S., Zdravković, L., Potts, D.M. and Salandy, N. E. (2007), "The Domain Reduction Method as an advanced boundary condition" in *4th International Conference on Earthquake Geotechnical Engineering*. Paper No. 1231. Greece.
11. Lysmer, J. and Kuhlemeyer, R. L. (1969), «Finite dynamic model for infinite media. *J. Eng. Mech. Div.* ASCE, Vol. 95(EM4):859-877.
12. Kuhlemeyer, R.L. and Lysmer, J. (1973), "Finite element method accuracy for wave propagation problems." *J. Soil Mech. Founds Div.* ASCE, Vol. 99: 421-427.
13. Maheshwari, B.K., Truman, K.Z., El Naggar, M.H. and Gould, P. L. (2004), "Three-dimensional finite element nonlinear dynamic analysis of pile groups for lateral transient and seismic excitations" *Can Geotech Jr.*, Vol. 41(1): 118-133.
14. Masing, G. (1926), *Eigenspannungen und Verfestigung beim Messing. Second International Congress on Applied Mechanics*, Zurich, Switzerland.
15. Mazzoni, S., McKenna, F., Scott, H. M. and Fenves, G. L. (2007), "The OpenSees command language manual", v6.0 <http://opensees.berkeley.edu>, Pacific Earthquake Engineering Research Center, University of California, Berkeley.
16. McCallen, D. B. and Romstad, K. M. (1994), "Analysis of a skewed short-span, box-girder overpass", *Earthquake Spectra* Vol. 10(4): 729-755.
17. McKenna, F., Fenves, G. L. (2008), "Using the OpenSees interpreter in Parallel Computers", University of California, Berkeley. NEESit; TN-2007-16, v1.0
18. Mokwa, R. L. and Duncan, J. M. (2000). "Investigation of the Resistance of Pile Caps and Integral Abutments to Lateral Loading." *Final Contract Report. Virginia Transportation Research Council*, Virginia Tech, Blacksburg, VA.
19. Prevost, J. H. (1985), "A Simple Plasticity Theory for

Frictional Cohesionless Soils”, *Soil Dyn. & Earthquake Eng.* Vol. 4(1): 9–17.

20. Pyke, R.M. (1979), “Nonlinear soil models for irregular cyclic loadings.” *Jr. Geotech. Engg. Div.*, ASCE; 105(GT6):715-726.
21. Seed, H. B., Ugas, C. and Lysmer, J. (1976), “Site dependent spectra for earthquake-resistant design”, *Bull. Seismol. Soc. Am.* Vol. 66(1): 221–243.
22. Smerzini, C., Galasso, C., Iervolino, I. and Paolucci, R. (2014), “Ground motion record selection based on broadband spectral compatibility”. *Earthquake Spectra*. Vol. 30(4): 1427–1448.
23. Smerzini, C., Paolucci, R., Galasso, C. and Iervolino, I. (2012), “Engineering ground motion selection based on displacement-spectrum compatibility”, in *Proceedings of the 15th World Conference on Earthquake Engineering*, Paper no. 2354. Lisbon, Portugal.
24. United States Geological Survey (USGS) (2008). *National Seismic hazard maps: documentation*. USGS Open File Report 2008-1128.
25. Vucetic, M. (1990), “Normalized behavior of clay under irregular cyclic loading”. *Can Geotech Jr.* 27(1): 29-46.
26. Zhang, Y., Conte, J.P., Yang, Z., Elgamal, A., Bielak, J. and Acero, G. (2008). “Two dimensional nonlinear earthquake response analysis of a bridge-foundation ground system,” *Earthquake Spectra*, Vol. 24(2): 343-386.